JOURNAL OF CATALYSIS 96, 439–453 (1985)

Syngas Reactions[1]

IX. Acetic Acid from Synthesis Gas

JOHN F. KNIFTON

Texaco Chemical Company, P.O. Box 15730, Austin, Texas 78761

Received April 30, 1985; revised June 26, 1985

Acetic acid has been generated directly from synthesis gas (CO/H_2) in up to 95 wt% selectivity and 97% carbon efficiency using a Ru–Co–I/Bu_4PBr "melt" catalyst combination. The critical roles of each of the ruthenium, cobalt, and iodide catalyst components in achieving maximum selectivity to HOAc have been identified. C_1-oxygenate formation is only observed in the presence of ruthenium carbonyls; $[Ru(CO)_3I_3]^-$ is here the dominant species. Controlled quantities of iodide ensure that initially formed MeOH is rapidly converted to the more reactive methyl iodide. Subsequent cobalt-catalyzed carbonylation to acetic acid may be preparatively attractive (>80% selectivity) relative to competing syntheses where the $[Co(CO)_4]^-$ concentration is maximized; that is, where the Co/Ru ratio is >1, the syngas feedstock is rich in CO and the initial iodide/cobalt ratios are close to unity. Formation of cobalt–iodide species in significant concentrations appears to be an inhibiting step in this synthesis.

INTRODUCTION

A major C_1 chemistry research effort has been underway in recent years directed toward the large-scale synthesis of acetic acid—as well as other commodity aliphatic oxygenates and hydrocarbons—from synthesis gas (*1*). In previous papers in this series we have described the application of ruthenium "melt" catalysis to the selective hydrogenation of CO to lower alkanols (*2, 3*), carboxylic acid esters, diols such as ethylene glycols (*4, 5*), as well as a two-step process for generating ethylene and related lower olefins (*6*). Here we describe a further application of ruthenium "melt" catalysis, wherein synthesis gas (CO/H_2) is for the first time converted directly to acetic acid in >80 wt% selectivity in the crude liquid product (*7, 8*).

$$2CO + 2H_2 \rightarrow CH_3COOH \qquad (1)$$

Ruthenium, cobalt, and halogen are the key elements of this catalysis (*7*), although ruthenium in combination with halogen-containing zirconium and titanium derivative is also effective (*8*). In the case of the Ru–Co couple, the highest yields of acetic acid can generally be achieved with ruthenium oxide, carbonyls, and complex derivatives in combination with various cobalt halides dispersed in low-melting quaternary phosphonium halide salts (*7*). A significant enhancement in both acetic acid productivity and selectivity is normally realized in the presence of controlled quantities of iodide.

Previous published work on the generation of acetic acid from syngas is generally confined to papers and patents disclosing the use of modified rhodium heterogeneous catalysts. Rhodium-on-silica alone (*9*), or in combination with manganese (*10*), ruthenium (*11*), molybdenum (*12*), and magnesium (*13*) promoters, yields acetic acid, ethanol, and acetaldehyde as the principal liquid-phase products. Wilson *et al.* (*14*) have employed a variety of rhodium-on-silica catalysts under conditions of low (<5%) CO conversions to produce two-carbon oxygenates, specifically acetic acid, acetaldehyde and ethanol, with carbon efficiencies

[1] For the previous paper in this series see: Knifton, J. F., *J. Mol. Catal.* **30**, 281 (1985).

0021-9517/85 $3.00

on the order of 50%. Methane is the principal by-product. The addition of 1% manganese to Rh/SiO_2 catalyst raises the synthesis rate about tenfold (*15*).

Recently, it has been reported by Kaplan that carbon monoxide reacts with aqueous HI to give acetic acid (*16*) and that carbon monoxide is catalytically converted to acetic acid and to glycolic acid by solutions containing acid (HCl or H_3PO_4) and compounds of palladium, rhodium, platinum, and iridium (*17*).

RESULTS

Data in Table 1 illustrate the production of acetic acid from 1/1 syngas catalyzed by ruthenium–cobalt halide bimetallic combinations dispersed in tetrabutylphosphonium bromide (m.p. 100°C).

The ruthenium(III) acetylacetonate–cobalt(II) iodide couple, for example, when dispersed in tetrabutylphosphonium bromide (Example 1) and treated with 1/1 CO/H_2 at 220°C, generates a liquid product containing 76 wt% acetic acid plus 1.1 wt% propionic acid (111 mmol total acid). The liquid yield increase is 66% and the estimated carbon selectivity to acetic plus propionic acids and their esters is 84%. There is normally no metallic residue at this stage (see Experimental), ruthenium and cobalt recovery is essentially quantitative at the end of the run, and the product acids may be recovered in >90% purity by fractional distillation. Methane and water are the major by-products (although in estimating carbon efficiency, the quantities of CO_2 formed as a result of water-gas shift activity (*2*) are not included)[2].

[2] All liquid organic products (acids, esters, and alkanols) plus methane have been considered in this work in estimating carbon efficiency for each of the individual experiments described in Table 1 and in the following figures. The quantity of CO_2 formed is included in Table 1, but is not considered in carbon selectivity calculations since this component can be readily recycled to the synthesis gas generator as a source of additional CO (see Ref. (*18*)). For previous examples of ruthenium-catalyzed water-gas shift activity in acidic media see Ref. (*19*).

Example 2 provides a further illustration of direct acetic acid synthesis. Here the concentration of acetic acid in the crude liquid product is 70 wt% and the estimated carbon efficiency to acetic acid, propionic acid, and their esters is 83%. Likewise, in the case of the 6-h run of example 3, the concentration of acetic acid in the liquid product is 69 wt%, carbon efficiency to acetic, propionic acids + esters is 87%, and the turnover frequency is 1.1×10^{-3} s^{-1} basis ruthenium charged.

A variety of ruthenium-containing precursors—coupled with cobalt halide, carbonate, and carbonyl compounds—at different initial Co/Ru atomic ratios, has been found to yield the desired carboxylic acids when dispersed in tetrabutylphosphonium bromide. Although the ruthenium–cobalt(II) iodide combination provides the highest selectivity to desired acetic acid (Examples 1 → 4), it has been unexpectedly found that the carbonylation activity of the $Ru\text{-}CoI_2$ couple is dramatically suppressed when additional iodide-containing promoters (such as methyl iodide and iodine, Examples 10 → 11) are introduced into the reaction media. This surprising feature is discussed in more detail *infra*.

In a more detailed examination of the ruthenium–cobalt–iodide "melt" catalyst system, we have followed the generation of acetic acid and its acetate esters as a function of catalyst composition and certain operating parameters, and examined the spectral properties of these reaction products, particularly with regard to the presence of identifiable metal carbonyl species.

A typical reaction profile is illustrated in Fig. 1 for the $Ru_3(CO)_{12}$–CoI_2/Bu_4PBr catalyst precursor. Under the selected operating conditions, acetic acid is the major product fraction; here it may comprise up to 85 wt% of the liquid product fraction (molar selectivity to HOAc is 86%, initial turnover frequency ca. 2.0×10^{-3} s^{-1} per g atom Ru charged). Methyl and ethyl acetates are also in evidence.

Figure 2 illustrates the effect of incre-

TABLE 1

Carboxylic Acids from Synthesis Gas[a,b]

Example	Catalyst precursor	Quaternary salt	Product composition (mmol)[c]								Liquid yield (%)
			CH_3COOH	C_2H_5COOH	CH_3COOMe	CH_3COOEt	CH_3COOPr	H_2O	CH_4	CO_2	
1	$Ru(acac)_3$–CoI_2	Bu_4PBr	110	1	2	9	2	20	53	432	66
2	RuO_2 –$2CoI_2$[d]	Bu_4PBr	33	5	0.2	4	2	7	22	317	24
3	$Ru_3(CO)_{12}$–CoI_2[e]	Bu_4PBr	58	0.4	3	9	2	10	18	129	41
4	$Ru_3(CO)_{12}$–CoI_2	Bu_4PBr	116	5	4	34	6	10	37	349	84
5	RuO_2 –$CoBr_2$	Bu_4PBr	132	2	32	81	20	25	156	1350	204
6	RuO_2 –$CoCl_2$	Bu_4PBr	50	7	39	66	11	382	678	2400	358[f]
7	RuO_2 –$CoCO_3$	Bu_4PBr	60	2	31	47	9	225	374	2640	299[g]
8	$Ru_3(CO)_{12}$–$Co_2(CO)_8$[h]	Bu_4PBr	34		2	5		6	1	10	29
9	RuO_2 –$Co_2(CO)_8$ –I_2	Bu_4PBr	113	3	6	23	6	19	122	972	108
10	RuO_2 –CoI_2 –I_2	Bu_4PBr	20			1	0.3	1	15	381	11
11	RuO_2 –CoI_2 –4MeI	Bu_4PBr							24	113	<2
12	CoI_2	Bu_4PBr									<2
13	$Ru_3(CO)_{12}$[e]	Bu_4PBr			23	16	3	14	141	518	192[i]

[a] Operating conditions: 482 bar; 220°C; 18 h; CO/H_2, 1 : 1.

[b] Reaction charge: Ru, 4.0 mmol; Co, 4.0 mmol; Bu_4PBr, 10.0 g.

[c] Analysis of gas and liquid samples by GLC; CH_3COOEt and CH_3COOPr fractions contain small quantities of C_2H_5COOMe and C_2H_5COOEt, respectively; liquid products may also contain smaller quantities of MeOH, EtOH, PrOH, MeOOCH, and $(CH_2OH)_2$.

[d] Reaction charge: Ru, 4.0 mmol; Co, 8.0 mmol.

[e] Run time, 6 h.

[f] Product also contains: MeOH, 150 mmol; EtOH, 136 mmol; PrOH, 29 mmol; liquid product comprises two phases.

[g] Product also contains: MeOH, 107 mmol; EtOH, 104 mmol; PrOH, 23 mmol.

[h] Run conditions: see Ref. (*2*).

[i] Product also contains: MeOH, 244 mmol; EtOH, 110 mmol; PrOH, 11 mmol.

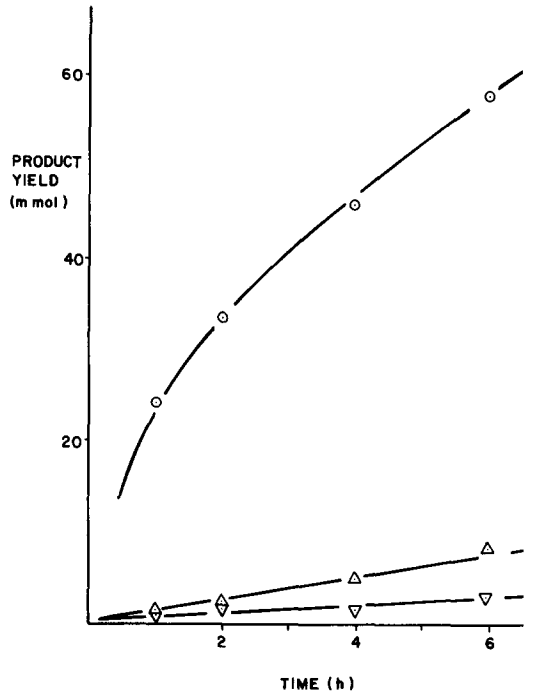

FIG. 1. Typical reaction profile. Reactor charge: $Ru_3(CO)_{12}$, 4.0 mmol Ru; CoI_2, 4.0 mmol Co; Bu_4PBr, 10.0 g; reaction conditions: 480 bar pressure; 220°C; 1:1 CO/H_2. CH_3COOH, ⊙; CH_3COOCH_3, ▽; $CH_3COOC_2H_5$, △.

mental changes in ruthenium catalyst content upon the production of acetic acid and its C_1–C_2 alkyl acetate esters. Acetic acid production is maximized at Ru/Co ratios of ca. 1 → 1.5, however, the data in Fig. 2 do show an approximate first-order dependence of ΣOAc^- (acetic acid plus acetate esters) upon initial ruthenium content, at least up to the 2/1, Ru/Co stoichiometry under the chosen conditions. Selectivity to acetic acid in the liquid product peaks at 92 wt% (carbon efficiency 95 mol%) for a catalyst combination with initially low Ru/Co ratios (e.g., 1:4). The formation of C_1–C_2 alkanols and their acetate esters rapidly exceeds acetic acid productivity when the Ru/Co atomic ratio is raised above 1.5, although two-carbon oxygenates continue to be the predominant fraction. Smaller quantities of glycol may be in evidence; CO_2 is a significant gas fraction.

The effect of varying cobalt concentration has been examined for two classes of catalyst precursor, viz. $Ru_3(CO)_{12}$–CoI_2/Bu_4PBr and $Ru_3(CO)_{12}$–$Co_2(CO)_8$–I_2/Bu_4PBr. The highest acetic acid selectivity in the liquid product (84%) was again achieved for both experimental series at Co/Ru molar ratios exceeding unity (see, for example, Fig. 3). Maximum ΣOAc^- content was achieved at Co/Ru ratios of ca. 0.5 (Fig. 3), while the highest turnover frequencies (5×10^{-3} s^{-1} per g atom Ru charged) were measured at CoI_2/Ru molar ratios of 1/4. No significant quantities of acetic acid are detected in the absence of the cobalt (see also Table 1, Example 13), although acetate esters may be generated in moderate yields, together with larger quantities of C_1–C_2 alkanol.

The presence of an iodide component appears to be essential to the formation of acetic acid in >70 wt% selectivity (*7*). A series of comparative experiments using a ruthenium–cobalt catalyst of the general composition $Ru_3(CO)_{12}$–$Co_2(CO)_8$–I_2/Bu_4PBr has been completed with different iodine contents. Selectivity to acetic acid reaches 95 wt% of the liquid product (97% carbon efficiency) for the Ru–Co–3I formulation (see Fig. 4). This is the highest HOAc selectivity achieved to date in this work. However, the heightened selectivity is generally realized at the expense of reactor productivity. Lower I/(Ru + Co) atomic ratios (e.g., 0.25) ensure a rise in productivity (turnover frequency 2.9×10^{-3} s^{-1} per g atom Ru), while HOAc selectivity dips to 10 wt% as methanol and homologation activity increases. Essentially no liquid oxygenates are formed as the initial I/(Ru + Co) atomic ratios approach two (see also Fig. 3 and Table 1, Example 11).

DISCUSSION

It is clear that ruthenium–cobalt–iodide catalyst dispersed in low-melting tetrabutylphosphonium bromide provides a unique means of selectively converting synthesis gas in one step to acetic acid. Modest

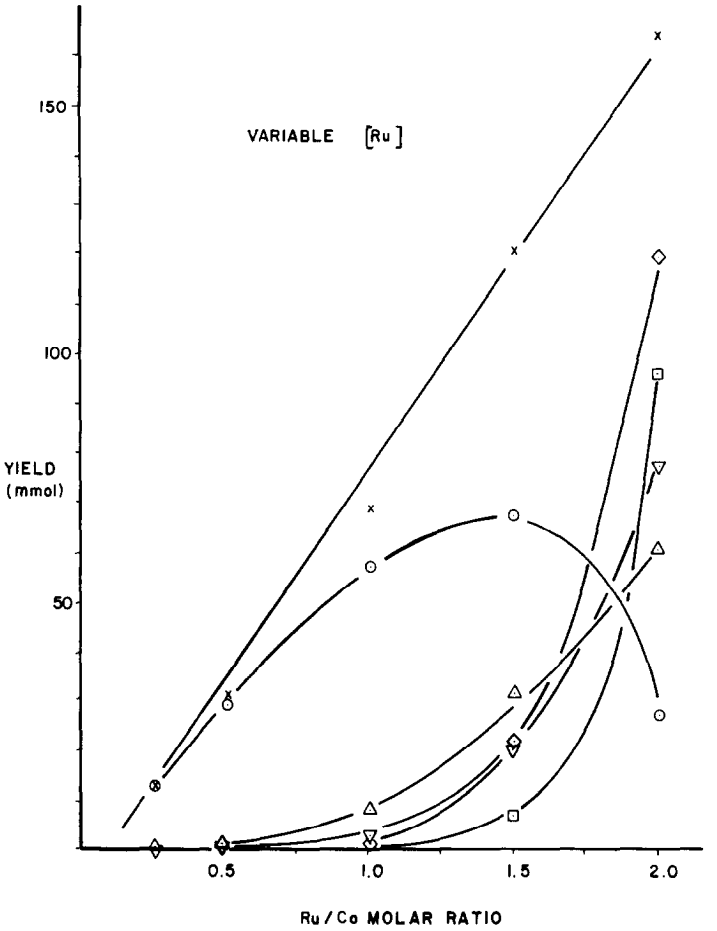

FIG. 2. Effect of varying [Ru]. Reactor charge: CoI_2, 4.0 mmol; Bu_4PBr, 10.0 g; reaction conditions as per Fig. 1; reaction time, 6 h. CH_3COOH, ⊙; CH_3COOCH_3, ▽; $CH_3COOC_2H_5$, △; ΣCH_3COO^-, ×; CH_3OH, ⊡; C_2H_5OH, ◇.

changes in catalyst formulation can, however, have profound effects upon liquid product composition.

Cobalt and iodide are the critical catalyst components that control the selectivity to desired acetic acid (Figs. 3 and 4) and under certain conditions they may also substantially alter the overall productivity to liquid oxygenates. The Ru–Co–3I/Bu_4PBr catalyst stoichiometry, for example, gives acetic acid in 95 wt% selectivity of the total liquid product (Fig. 4), and while carbon efficiency to HOAc is estimated to be 97 mol%, the CO hydrogenation rate is only ca. 0.2×10^{-3} s^{-1} per g atom Ru charged. Turnover frequency, by contrast, may reach 5.0×10^{-3} s^{-1} per g atom Ru charged for a somewhat similar $Ru_3(CO)_{12}$–CoI_2/Bu_4PBr catalyst formulation (Ru : Co, 1 : 4) where acetic acid selectivity is significantly lower (see Fig. 3).

Generally, CO hydrogenation catalyzed by iodide-free ruthenium–cobalt "melt" catalysis leads to the formation of liquid oxygenates through at least four competing reactions (*2*), viz.: methanol generation, methanol homologation, methanol carbonylation to acetic acid, and acid esterification with product alkanols. Methanol, ethanol, and ethylene glycol generation do not require a cobalt catalyst component (*4, 5*) or the presence of iodide. The introduction

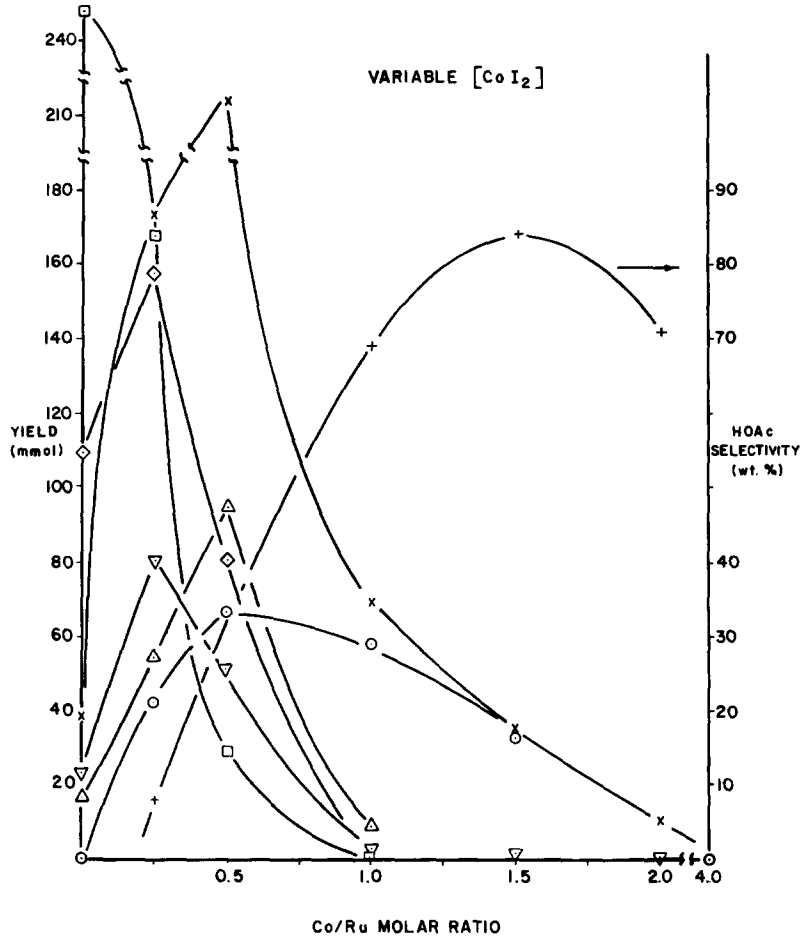

FIG. 3. Effect of varying [CoI_2]. Reactor charge: $Ru_3(CO)_{12}$, 4.0 mmol Ru; Bu_4PBr, 10.0 g; reaction conditions as per Fig. 1; reaction time, 6 h. Legend as per Figs. 1 and 2, HOAc selectivity, +.

of a cobalt component (*2*) generally leads to (a) increased carbonylation activity and the formation of acetic acid; (b) the presence of $[Co(CO)_4]^-$ as a dominant cobalt species in solution; and (c) increased methanol homologation activity such that ethanol may become the major liquid oxygenate product fraction (*3*).

Although analogous relationships exist for the ruthenium–cobalt iodide/quaternary phosphonium salt catalysts examined in this work, there are critical differences; by careful control of the Ru : Co : I atomic ratios, this new class of catalyst can generate acetic acid in >90 wt% selectivity in the liquid phase with little or no alkanol by-product formation.

The new data illustrate how preparatively attractive yields of acetic acid (and maximum rates of HOAc formation) may be realized with the "melt" catalyst system when the following criteria are met:

(a) ruthenium–cobalt atomic ratios range from ca. 0.5 : 1 → 2 : 1 (see Figs. 2 and 3); (b) transition metal–iodide ratios (Ru : Co : I) are ca. 1 : 1 : 1 (Fig. 4); and (c) carbon monoxide partial pressures exceed ca. 70 bar (Fig. 5).

Spectroscopic studies of typical $Ru_3(CO)_{12}$–$Co_2(CO)_8$–I_2/Bu_4PBr catalyst solutions have served to aid considerably in unraveling the differing roles of the ruthenium-, cobalt-, and iodide-containing catalyst components in these syntheses. A

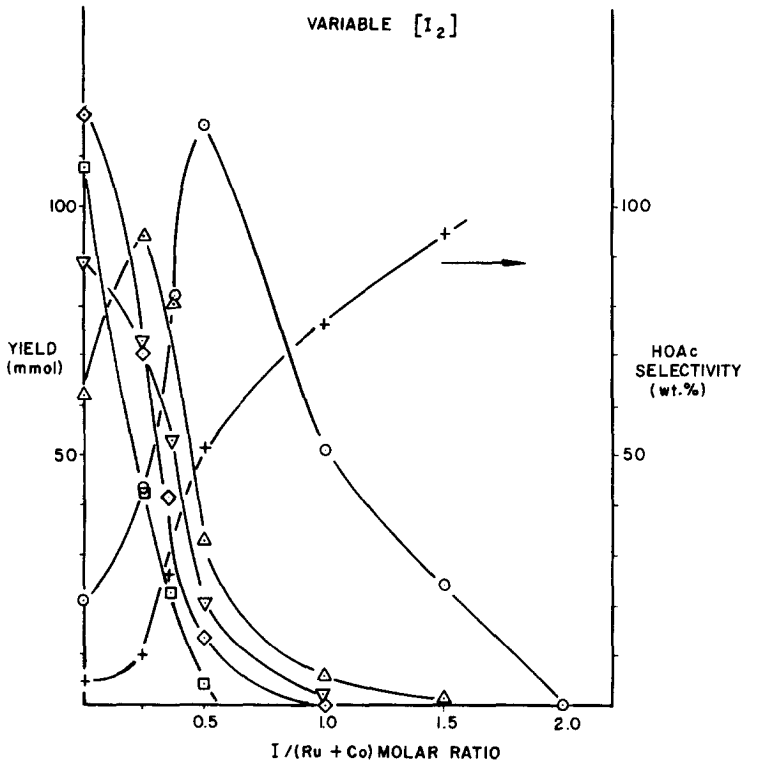

FIG. 4. Effect of varying $[I_2]$. Reactor charge: $Ru_3(CO)_{12}$, 4.0 mmol Ru; $Co_2(CO)_8$, 4.0 mmol Co; Bu_4PBr, 10.0 g; reaction conditions as per Fig. 1; reaction time, 6 h. Legend as per Figs. 1 and 2, HOAc selectivity, +.

typical solution spectrum in the metal–carbonyl region (Fig. 6) shows the presence of significant concentrations of both $[Ru(CO)_3I_3]^-$ (2108 and 2036 cm^{-1}) and $[Co(CO)_4]^-$ (1886 cm^{-1}, see Refs. (*20, 21*)). Most of the ruthenium charged can be accounted for on the basis of the strength of the $[Ru(CO)_3I_3]^-$ absorptions. The importance of this species to the CO hydrogenation syntheses is evident from the close parallel we find between the yields of liquid oxygenate and acetic acid (ΣOAc^-), and the increase in ruthenium carbonyl iodide, $[Ru(CO)_3I_3]^-$, content—as determined by its characteristic absorption at 2036 cm^{-1}. The relationships are illustrated in Fig. 7. NMR spectra of these typical product solutions show no hydride signals to δ −20 ppm. As in Table 1, Example 12, no aliphatic oxygenates are formed in the absence of the ruthenium catalyst component. The data (particularly the relationships of Figs. 2 and 7) are in keeping with our earlier spectral correlations (*2*), pointing to initial C_1-oxygenate (methanol) formation being associated with the presence of the $[Ru(CO)_3X_3]^-$ anion. This same monomeric ruthenium(II) carbonyl is dominant in related ruthenium-catalyzed acetate ester (*22*) and carboxylic acid (*23*) synthesis, and is critical to the facile generation of ethylene glycol and monohydric alkanols from CO/H_2 (*24*). Nevertheless, these data do not preclude the formation of spectroscopically undetectable derivatives of $[Ru(CO)_3I_3]^-$, that are more reactive electrophilic and nucleophilic intermediates, and the truly catalytically active components of these syntheses under steady-state conditions. Chromatographic separation of the crude liquid products from Table 1, Examples 1–4 failed to yield other identifiable

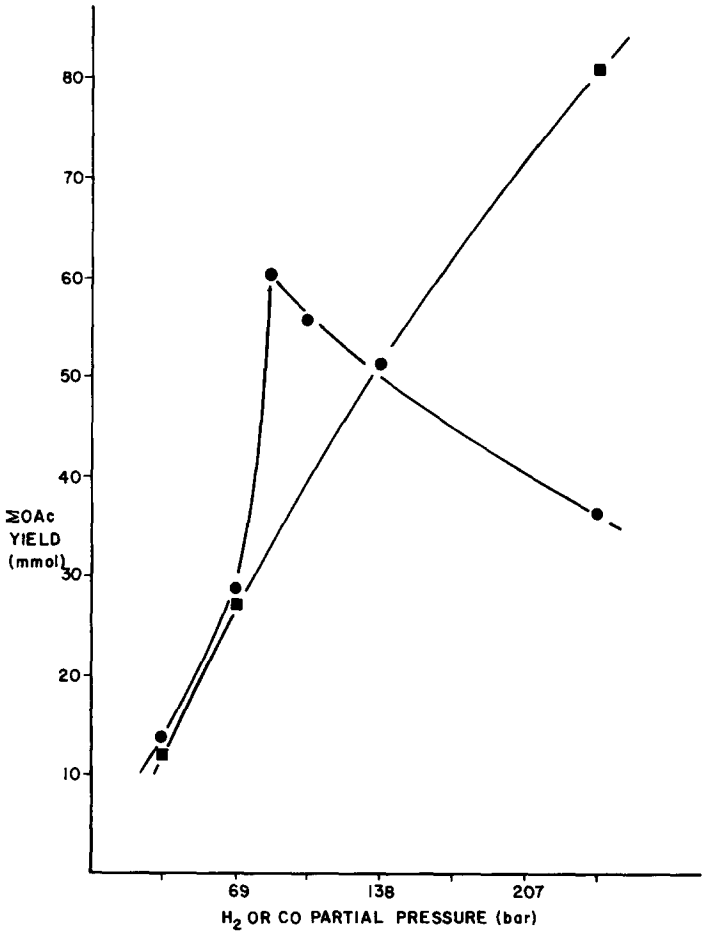

FIG. 5. ΣOAc versus carbon monoxide partial pressure. Reactor charge: $Ru_3(CO)_{12}$–CoI_2/Bu_4PBr as per Fig. 1; reaction conditions: 138 bar H_2; 220°C; 6 h, ●; reactor conditions: 138 bar CO; 220°C; 6 h, ■.

mononuclear ruthenium carbonyls in the highly polar "melt" media, although there is tentative evidence for the presence of the cluster anion $[Ru_3(CO)_{11}]^{2-}$. Anionic ruthenium hydridocarbonyls of higher nuclearity, e.g. $[HRu_3(CO)_{11}]^-$, can be detected spectroscopically, but only at low iodide content, where acetic acid selectivity is poor (<20%), and alkanols are the predominant products (*2, 4*) (see Figs. 3 and 4).

Regarding the function of the cobalt component, we find for different iodide charges (at fixed Ru, Co) there is a close parallel between HOAc productivity and the presence of the cobalt carbonyls, and a linear relationship between ΣOAc^- and $[Co(CO)_4]^-$ anion content (see Fig. 8). This linear correspondence, taken together with the [Co], HOAc selectivity correlation of Fig. 3, is indicative of cobalt carbonyl—or a derivative thereof—being responsible for the formation of the desired acetic acid.

Additional evidence regarding the role played by the cobalt carbonyl in the carbonylation sequence comes from the following observations.

(1) Acetic acid may be readily synthesized from methanol (Eq. (2)) in the absence of ruthenium, in 96% selectivity, using the $Co_2(CO)_8$–I_2/Bu_4PBr "melt" catalyst alone; the rate of this cobalt-catalyzed carbonylation is >3 times faster than the rate of acetic acid formation via reaction (1) using the Ru–Co–I/Bu_4PBr couple.

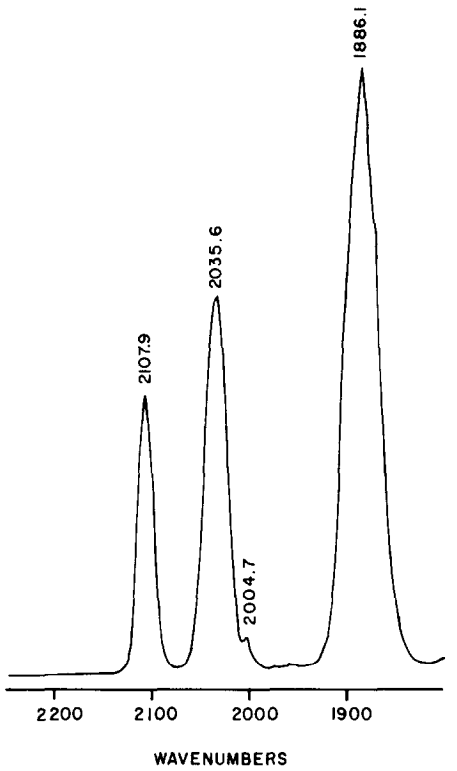

FIG. 6. Acetic acid from synthesis gas. Spectrum of typical product solution. Catalyst, $Ru_3(CO)_{12}$–$Co_2(CO)_8$–I_2/Bu_4PBr.

Similarly, acetic acid may be generated from methyl iodide using cobalt octacarbonyl-tetrabutylphosphonium bromide as catalyst precursor.

(2) Starting from ^{13}C-enriched methanol, the $Co_2(CO)_8$–I_2/Bu_4PBr "melt" catalyst carbonylates to acetic acid in accord with Eq. (2), enrichment being detected only on the methyl carbon.

$$\overset{*}{C}H_3OH + CO \rightarrow \overset{*}{C}H_3COOH \qquad (2)$$

(3) In competitive experiments, although $Ru_3(CO)_{12}/Bu_4PBr$ and its cobalt-containing analog, $Ru_3(CO)_{12}$–CoI_2/Bu_4PBr, both exhibit rapid rates of ΣC_1 oxygenate formation, the yield of HOAc is a factor of $>10^2$ higher for the Ru–Co combination (see Table 1, cf. Examples 3 and 13, and Fig. 3). Cobalt—in the absence of ruthenium—does not, on the other hand, convert syngas to liquid oxygenates (Table 1, Example 12).

Regarding the sensitivity of HOAc selectivity to catalyst structure, we find that preparatively attractive selectivities to acetic acid (>80 wt%) in the liquid product may be realized for the Ru–Co–I/Bu_4PBr "melt" catalysts when the following general conditions are met: (a) cobalt : ruthenium atomic ratios are ca. unity or greater (see Figs. 2 and 3); (b) iodide/(Ru + Co) ratios are ca. 1.5 : 1 or greater (Fig. 4); and (c) the synthesis gas feedstock is rich in CO (Fig. 9).

For example, at fixed ruthenium content, increases in cobalt charge lead to significant changes in $[Co(CO)_4]^-$ content, and for both the $Ru_3(CO)_{12}$–CoI_2/Bu_4PBr and $Ru_3(CO)_{12}$–I_2/Bu_4PBr formulations, there is a linear correlation between acetic acid selectivity and changes in $[Co(CO)_4]^-$ content (over limited [Co], see Fig. 10). This relationship provides further evidence implicating the cobalt carbonyls—or their derivatives—as responsible for the carbonylation activity leading to HOAc formation.

Nevertheless, the critical role of the iodide fraction in ensuring a selective acetic acid synthesis is illustrated by the data in Fig. 4. Here it can be seen that the introduction of controlled quantities of iodide component may bring about a greater than 20-fold improvement in acetic acid selectivity (from 4.3 to 94.8 wt%) in the liquid product. While the acetic acid productivity peaks at I/Co ratios of ca. unity, a further increase in this ratio dramatically lowers the HOAc productivity so that by 4/1 there is essentially no liquid product. Significantly, at this I/Co ratio, the infrared spectrum of the catalyst complex shows essentially complete elimination of the absorption at 1886 cm^{-1} due to $[Co(CO)_4]^-$, while the presence of $[CoI_4]^{2-}$ is confirmed by its characteristic (*25*) strong absorption in the visible spectrum at ca. 700 μm. Chromatographic separation of these crude liquid products allows isolation of fractions containing $[CoI_4]^{2-}$. Once again then, carbonylation activity leading to acetic acid tracks the presence of cobalt tetracarbonyl

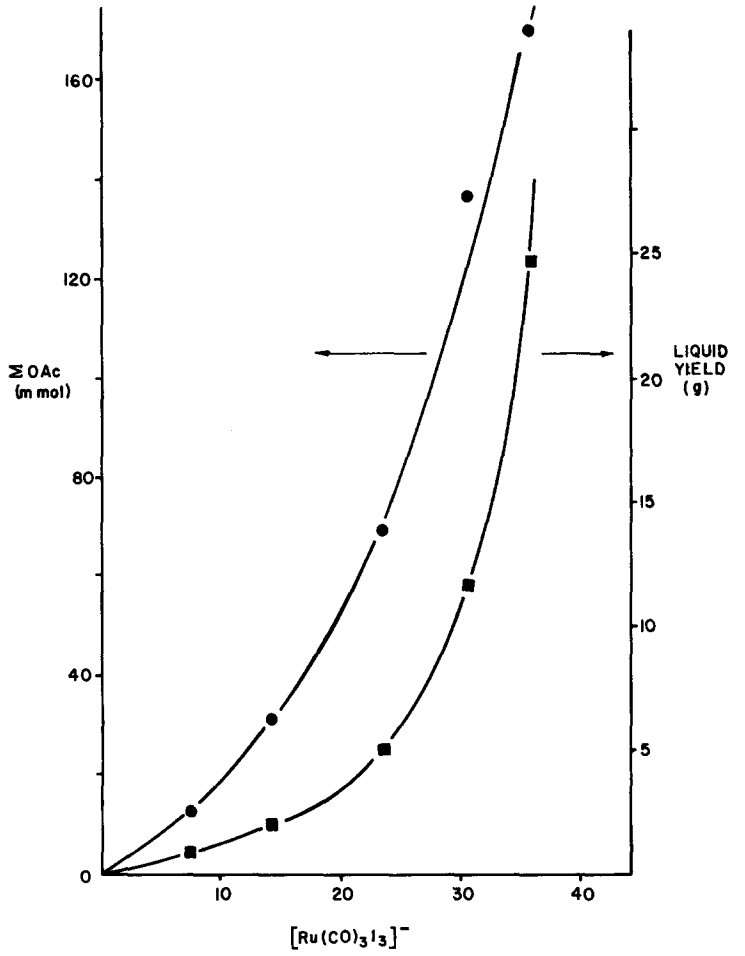

FIG. 7. ΣOAc and liquid yield versus $[Ru(CO)_3I_3]^-$. Reactor charge and conditions as per Fig. 2.

anion. Somewhat similar observations have been reported for cobalt–iodide-catalyzed methanol homologation (*26*).

To achieve, then, high acetic acid selectivity directly from synthesis gas (Eq. (1)) it is necessary to balance the rates of the two consecutive steps of this preparation—ruthenium–carbonyl-catalyzed methanol formation (*4*) (Figs. 2 and 7) and cobalt–carbonyl-catalyzed carbonylation to acetic acid (Figs. 8 and 10)—such that the instantaneous concentration of methanol does not build to the level where competing secondary reactions, particularly methanol homologation (*23, 27*), ester homologation (*28, 29*), and acid esterification (*22*), become important.

The iodide content of the catalyst formulation is the key to avoiding these problems of competing reactions and achieving maximum acetic acid selectivity. The addition of iodide ensures that any initially formed methanol (*2*) (Scheme 1) is rapidly (*27*) converted to the more electrophilic methyl iodide. Cobalt-catalyzed carbonylation (presumably via the oxidative addition of the newly formed CH_3I to $Co(CO)_4^-$ to yield $CH_3Co(CO)_4$ (*30*), step C) then proceeds via migratory insertion (step D) (*31*) to acetic acid, thereby significantly improving HOAc selectivity (Fig. 4) by avoiding alternative MeOH conversion paths to C_2-oxygenates, such as homologation and esterification. Nevertheless, further increases in

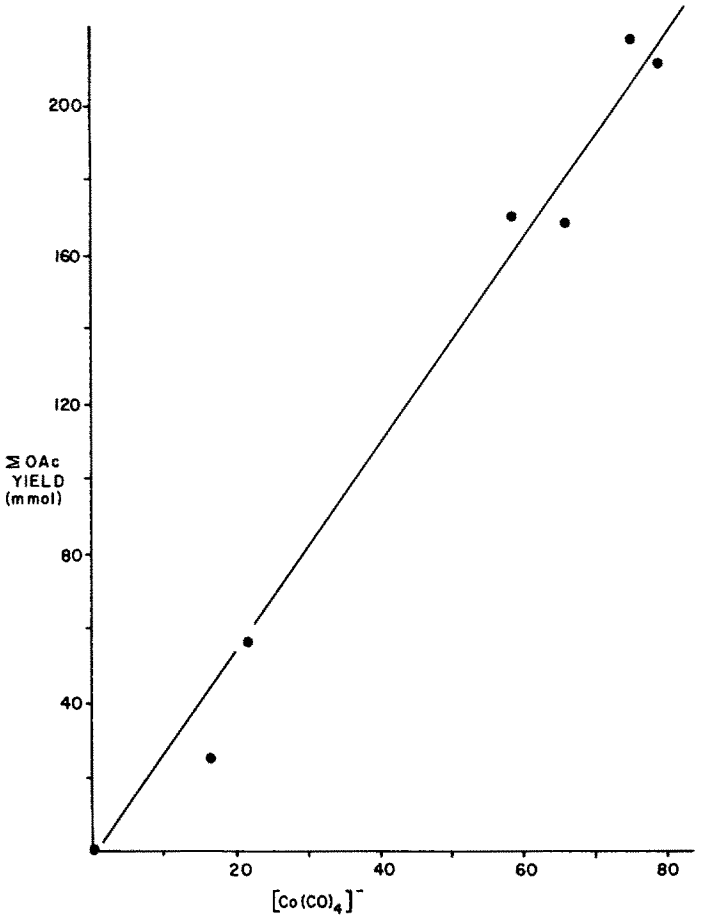

FIG. 8. ΣOAc versus $[Co(CO)_4]^-$. Reactor charge and conditions as per Fig. 4.

$$CO/H_2 \xrightarrow{Ru} Ru\text{-}\overset{O}{\overset{\|}{C}}H \xrightarrow{H_2} Ru\text{-}CH_2OH \xrightarrow[-Ru]{H_2} CH_3OH \qquad (A)$$

$$CH_3OH + HI \longrightarrow CH_3I + H_2O \qquad (B)$$

$$CH_3I + Co(CO)_4^- \rightleftharpoons CH_3Co(CO)_4 + I^- \qquad (C)$$

$$CH_3Co(CO)_4 \xrightleftharpoons{CO} CH_3\overset{O}{\overset{\|}{C}}Co(CO)_4 \qquad (D)$$

$$CH_3\overset{O}{\overset{\|}{C}}Co(CO)_4 + H_2O \longrightarrow CH_3COOH + HCo(CO)_4 \qquad (E)$$

SCHEME 1

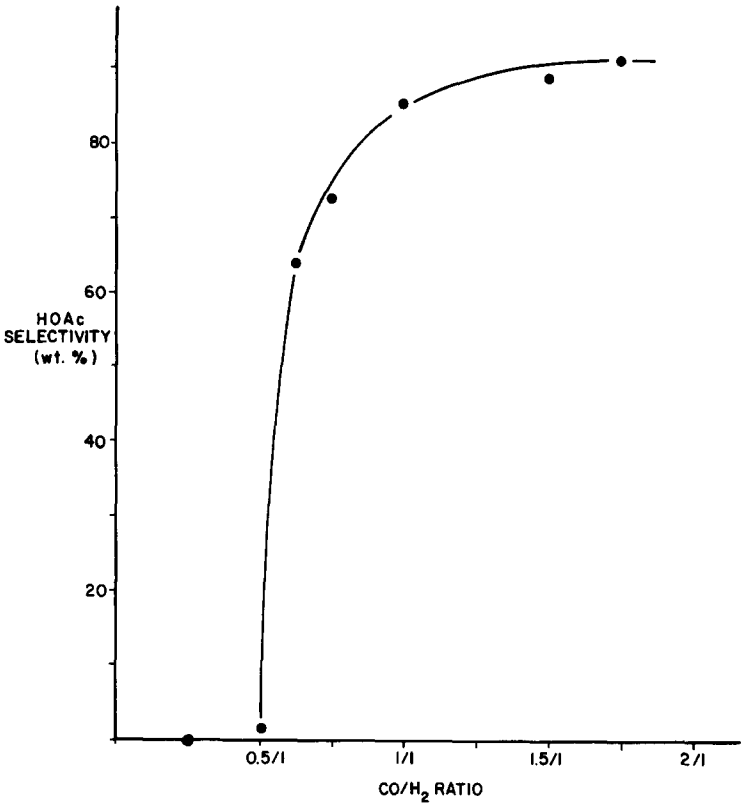

FIG. 9. HOAc selectivity versus syngas composition. Reactor charge and conditions as per Fig. 5.

the quantities of iodide beyond that needed for methanol conversion to methyl iodide (step B) may lead to a portion, or all, of the catalytically active cobalt carbonyl reverting to catalytically inactive cobalt iodide species, e.g., the $[CoI_4]^{2-}$ anion (see Eq. (3), Ref. (*32*)) identified in this work, or possibly the cationic $[Co(MeOH)_x(CO)_yI_z]^{n+}$ species[3] proposed earlier by Pretzer and Kobylinski for their cobalt–iodide-catalyzed homologation of methanol (*26*). The effect of this drop in $[Co(CO)_4]^-$ content is a dramatic lowering of the overall rate of carbonylation (see Figs. 4 and 10). The increase in HOAc yield with initial increased iodide content (I/Co ratio <1) and the typical decrease in HOAc yield at higher I/Co ratios are well illustrated by the graphs in Fig. 4. Methanol, ethanol, and acetate esters tend to predominate only at the lower iodide concentrations and lower I/Co molar ratios.

$$2[Co(CO)_4]^- + 3I_2 \rightarrow 2CoI_2 + 8CO + 2I^- \quad (3)$$

As in related cobalt-catalyzed methanol carbonylation processes (Eq. 2)[4] the production of HOAc is favored by high CO partial pressures (Fig. 5) and a CO-rich environment (Fig. 9) and it is likely that in both processes carbon monoxide is involved in the rate-limiting step (Scheme 1, step D). The complex, nonlinear, dependences upon CO and H_2 partial pressures (Fig. 5) are indicative of pressure-depen-

[3] Pretzer and Kobylinski (Ref. (*26*)) report absorption bands attributable to the $[Co(MeOH)_x(CO)_yI]^{n+}$ species at 2050, 2035, and 2010 cm^{-1}. In our work the strong band at 2036 cm^{-1} due to $[Ru(CO)_3I_3]^-$ masks the two higher energy bands, but a weak absorption at 2005 cm^{-1} (see Fig. 6) may be due to this species.

[4] Reaction conditions and Ru–Co catalyst charge as per Fig. 1.

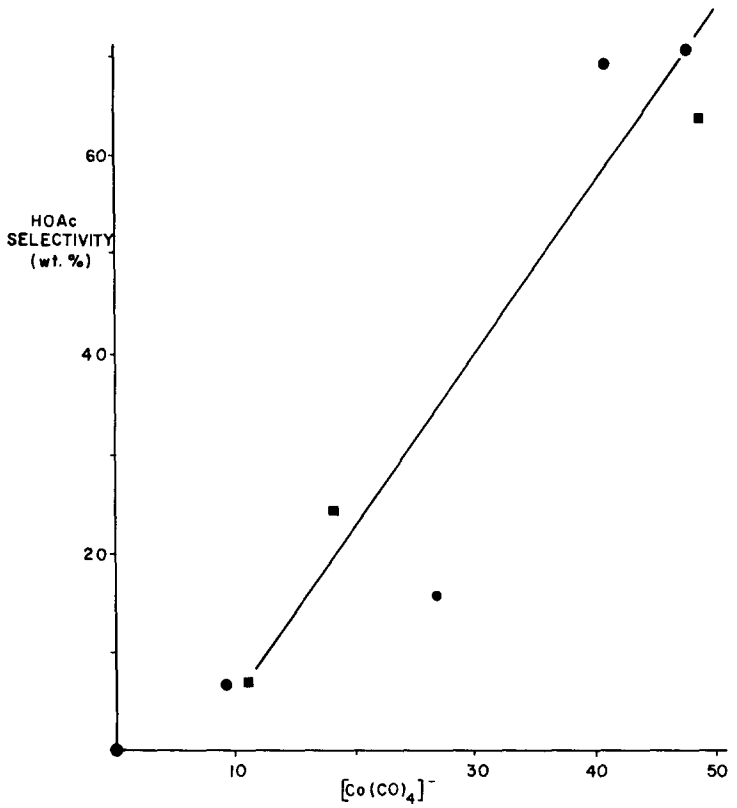

FIG. 10. HOAc selectivity versus $[Co(CO)_4]^-$. Catalyst precursor $Ru_3(CO)_{12}$–CoI_2/Bu_4PBr, reaction conditions as per Fig. 3, ●; catalyst precursor $Ru_3(CO)_{12}$–$Co(CO)_8$–I_2/Bu_4PBr, reaction charge: $Ru_3(CO)_{12}$, 4.0 mmol Ru; $Co_2(CO)_8$, 1–8 mmol Co; I, 4.0 mmol; Bu_4PBr, 10.0 g; reaction conditions as per Fig. 1, ■.

dent metal carbonyl equilibria involving either, or both, the Ru and Co metal centers. A lowering of P_{CO} (<85 bar), in particular, can be seen to alter the ruthenium nuclearity, so that both ruthenium(II), $[Ru(CO)_3I_3]^-$ (Fig. 6), and $[HRu_3(CO)_{11}]^-$ (Ref. (*2*)) may be detected spectroscopically.

An apparent activation energy of ca. 31 kcal mol^{-1} has been estimated in this work from an Arrhenius plot of ΣOAc^- versus temperature (200–240°C).[4] An Arrhenius plot for the cobalt-catalyzed methanol carbonylation process (Eq. (2)) is reportedly nonlinear (*33*), but the activation energy measured here is notably higher than the 14.7 kcal mol^{-1} reported (*34*) for the rhodium-catalyzed methanol carbonylation, or the 19 kcal mol^{-1} in ketonic solvents (*35*).

A migratory CO insertion mechanism for initial methanol formation, as depicted in Scheme 1 (involving the intermediate formation of labile ruthenium–formyl (*36–39*) and –hydroxymethyl (*40, 41*) complexes), is in keeping with our earlier kinetic and spectroscopic studies for the related $Ru_3(CO)_{12}$–$Co_2(CO)_8$/Bu_4PBr "melt" catalyst system (*2*). In that work, initial methanol formation was found to be first order in [Ru], linearly dependently upon CO partial pressure and qualitatively dependent upon the presence of $[Ru(CO)_3Br_3]^-$. In the present study, the sensitivity of methanol formation to [Ru] can be seen in Fig. 2, while the formation of minor quantities of methyl formate and ethylene glycol (Table 1) points to the importance of intermediate metal–methoxy and –hydroxymethyl species (*2, 42*).

Methane formation (Table 1, column 10) is believed to result primarily from hydrogenolysis of labile methyl–metal intermediates (*2, 23*) (e.g., from step C, Scheme 1). This has been established in experiments similar to Eq. (2), where, for the Ru–Co–I catalyst precursors, product methane containing the ^{13}C label is confirmed by gas-phase infrared spectroscopy (Eq. (4)). A similar result has been reported by Warren and Dombek (*24*) during ethanol generation from CO/H_2 via homogeneous ruthenium catalysis in the presence of an iodide promoter. Under our preferred HOAc synthesis conditions (*7*), there is no evidence for metal precipitates (vide supra) and methane formation is not considered to be heterogeneously catalyzed.

$$\overset{*}{C}H_3OH \xrightarrow{CO/H_2} \overset{*}{C}H_4 \qquad (4)$$

In conclusion then, it is evident from the data presented supra, that each of the ruthenium-, cobalt-, and iodide-containing species have very specific roles to play in the "melt" catalyzed conversion of synthesis gas to acetic acid. C_1-oxygenate formation is only observed in the presence of ruthenium carbonyls—$[Ru(CO)_3I_3]^-$ is here the dominant species and there is a direct relationship between liquid yield, ΣOAc^- productivity and $[Ru(CO)_3I_3]^-$ content (see Figs. 2 and 7). Controlled quantities of iodide ensure that initially formed MeOH is rapidly converted to the more reactive methyl iodide. Subsequent cobalt-catalyzed carbonylation to acetic acid may be preparatively attractive (>80% selectivity, good yields) relative to competing syntheses, where the $[Co(CO)_4]^-$ concentration is maximized (Figs. 8 and 10); that is, where the Co/Ru ratio is >1, the syngas feedstock is rich in CO, and the initial iodide/cobalt ratios are ca. unity. Formation of cobalt–iodide species appears to be a competing, inhibitory, step in this catalysis.

EXPERIMENTAL

Triruthenium dodecacarbonyl, cobalt(II) iodide hydrate and related metal oxides, salts and complexes were purchased from outside suppliers. Tetrabutylphosphonium bromide was purchased from Aldrich Chemical Company and used as received. Synthesis gas was supplied by Big Three Industries in various proportions of carbon monoxide and hydrogen. All high-pressure experiments were conducted in an 845-ml capacity Aminco pressure reactor constructed of 316 stainless steel, fitted with heating and agitation means, and hooked to a large, high-pressure synthesis gas reservoir. The reactor was always used with interchangeable Pyrex glass liners.

The extent of reaction and distribution of products was determined by gas–liquid chromatography. Acetic acid and propionic acid products, as well as their esters, were isolated by fractional distillation *in vacuo,* or by GLC trapping and identified by one of the following techniques, GLC, FTIR, NMR, and elemental analyses. Minor by-products were identified by GLC–FTIR or GLC–MS.

Acetic Acid Synthesis

A mixture of triruthenium dodecacarbonyl (4.0 mmol Ru, 0.852 g) and cobalt iodide (4.0 mmol, 1.395 g) dispersed in tetrabutylphosphonium bromide (10.0 g) is transferred to a glass liner, under N_2 purge, to an 845-ml capacity pressure reactor equipped with heating and means of agitation. The reactor is sealed, flushed with CO/H_2, and pressured to 138 bar with 1/1 CO/H_2. The mixture is heated to 220°C with rocking, the pressure raised to 482 bar by CO/H_2 from a large surge tank, and the reactor held at temperature for 18 h. Pressure in the reactor is maintained at ca. 480 bar by incremental additions of CO/H_2 from the surge tank.

On cooling, the reactor pressure (281 bar) is noted, typical gas samples taken, and the excess gas removed. The emerald-green liquid product (22.5 g) shows no evidence of a solid fraction. Samples are analyzed by GLC and Karl-Fischer titration. Typical data are 67.5 wt% acetic acid, 3.3 wt% propionic acid, 2.8 wt% methyl acetate, 15.3 wt% ethyl acetate, 5.8 wt% propyl acetate,

and 0.7 wt% water. Analyses of typical off-gas samples show the presence of 50% hydrogen, 44% carbon monoxide, 4.7% carbon dioxide, and 0.5% methane. Liquid yield is (22.5–12.2/12.2) × 100 = 84%.

The product acids and esters may be recovered from the crude liquid by fractional distillation. The residual tetrabutylphosphonium bromide salt shows no change in structure of the Bu_4P^+ unit—basis ^{31}P and ^{13}C analyses. Some halide exchange with the iodide component of the Ru–Co catalyst is evident from the characteristic[5] IR spectral bands in the region 2800–3000 cm^{-1} and at ca. 900 cm^{-1}.

ACKNOWLEDGMENTS

The author wishes to thank Texaco Inc. for permission to publish this paper, Messrs. M. R. Swenson, R. Gonzales, R. D. Czimskey, and D. W. White for experimental assistance, and Messrs. J. M. Schuster and C. L. LeBas for FTIR and NMR data.

REFERENCES

1. (a) Haggin, J., *Chem. Eng. News,* June 8, 1981, p. 23; (b) November 16, 1981, p. 57.
2. Knifton, J. F., Grigsby, R. A., and Lin, J. J., *Organometallics* **3,** 62 (1984).
3. Knifton, J. F., Grigsby, R. A., and Herbstman, S., *Hydrocarbon Process.,* January 1984, p. 111.
4. Knifton, J. F., *J. Amer. Chem. Soc.* **103,** 3959 (1981).
5. Knifton, J. F., *J. Chem. Soc. Chem. Commun.,* 729 (1983).
6. Knifton, J. F., *J. Catal.* **79,** 147 (1983).
7. Knifton, J. F., and Lin, J. J., U.S. Patent 4,366,259 to Texaco Develop. Corp. (1982).
8. Knifton, J. F., U.S. Patent 4,362,822 to Texaco Develop. Corp. (1982).
9. Bhasin, M. M., and O'Conner, G. L., U.S. Patent 4,246,186 to Union Carbide Corp. (1981).
10. Ellgen, P. C., and Bhasin, M. M., U.S. Patent 4,014,913 to Union Carbide Corp. (1977).
11. Hwang, H. S., and Taylor, P. D., U.S. Patents 4,101,450 (1978) and 4,136,104 (1979) to Celanese Corp.
12. Ellgen, P. C., and Bhasin, M. M., U.S. Patent 4,096,164 to Union Carbide Corp. (1978).
13. Wunder, F. A., Arpe, H. J., Leupold, E. I., and Schmidt, H. J., German Offen. 28,14,427 (1979) and 28,14,365 (1979) to Hoechst AG.
14. Bhasin, M. M., Bartley, W. J., Ellgen, P. C., and Wilson, T. P., *J. Catal.* **54,** 120 (1978).
15. Ellgen, P. C., Bartley, W. J., Bhasin, M. M., and Wilson, T. P., *in* "Hydrocarbon Synthesis from Carbon Monoxide and Hydrogen" (E. L. Kugler and F. W. Steffgen, Eds.), Advances in Chemistry Series 178, p. 147. Amer. Chem. Soc., Washington, D.C., 1979.
16. Kaplan, L., *J. Org. Chem.* **47,** 5422 (1982).
17. Kaplan, L., *J. Org. Chem.* **47,** 5424 (1982).
18. *Chem. Eng. News,* Nov. 12, 1984, p. 29.
19. Yarrow, P., Cohen, H., Ungermann, C., Vandenberg, D., and Ford, P. C., *J. Mol. Catal.* **22,** 239 (1983).
20. Cleare, M. J., and Griffith, W. P., *J. Chem. Soc. A,* 372 (1969).
21. Friedel, R. A., Wender, I., Shufler, S. L., and Sternberg, H. W., *J. Amer. Chem. Soc.* **77,** 3951 (1955).
22. Braca, G., Paladini, L., Sbrana, G., Valentini, G., Andrich, G., and Gregorio, G., *Ind. Eng. Chem. Prod. Res. Dev.* **20,** 115 (1981).
23. Knifton, J. F., *J. Mol. Catal.* **11,** 91 (1981).
24. Warren, B. K., and Dombek, B. D., *J. Catal.* **79,** 334 (1983); Dombek, B. D., *J. Organomet. Chem.* **250,** 467 (1983).
25. Mizoroki, T., and Nakayama, M., *Bull. Chem. Soc. Jpn.* **38,** 1876 (1965).
26. Pretzer, W. R., and Kobylinski, T. P., *Ann. N.Y. Acad. Sci.* **333,** 58 (1980).
27. Fakley, M. E., and Head, R. A., *Appl. Catal.* **5,** 3 (1983).
28. Braca, G., Sbrana, G., Valentini, G., and Cini, M., *J. Mol. Catal.* **17,** 323 (1982).
29. Hidai, M., Koyasu, Y., Yokota, M., Orisaku, M., and Uchida, Y., *Bull. Chem. Soc. Jpn.* **55,** 3951 (1982).
30. Heck, R. F., and Breslow, D. S., *J. Amer. Chem. Soc.* **84,** 2499 (1962).
31. Mizoroki, T., and Nakayama, M., *Bull. Chem. Soc. Jpn.* **39,** 1477 (1966); Galamb, V., and Palyi, G., *Coord. Chem. Rev.* **59,** 203 (1984).
32. Orchin, M., *in* "Advances in Catalysis," Vol. 5, p. 385. Academic Press, New York, 1953.
33. Mizoroki, T., Nakayama, M., and Furumi, M., *Kogyo Kagaku Zasshi* **65,** 1054 (1962).
34. Hjortkjaer, J., and Jensen, V. W., *Ind. Eng. Chem. Prod. Res. Dev.* **15,** 46 (1976).
35. Matsumoto, T., Mori, K., Mizoroki, T., and Ozaki, A., *Bull. Chem. Soc. Jpn.* **50,** 2337 (1977).
36. Schoening, R. C., Vidal, J. L., and Fiato, R. A., *J. Mol. Catal.* **13,** 83 (1981).
37. Pruett, R. L., Schoening, R. C., Vidal, J. L., and Fiato, R. A., *J. Organomet. Chem.* **182,** C57 (1979).
38. Holmgren, J. S., and Shapley, J. R., *Organometallics* **3,** 1322 (1984).
39. Sumner, C. E., and Nelson, G. O., *J. Amer. Chem. Soc.* **106,** 432 (1984).
40. Lin, Y. C., Milstein, D., and Wreford, S. S., *Organometallics* **2,** 1461 (1983).
41. Nelson, G. O., *Organometallics* **2,** 1474 (1983).
42. Costa, L. C., *Catal. Rev.-Sci. Eng.* **25,** 325 (1983).

[5] Infrared spectra of commercial samples of tetrabutylphosphonium bromide and tetrabutylphosphonium iodide were employed here as standards.